

Fabrication of Sn-Ni alloy film anode for Li-ion batteries by electrochemical deposition

ZHANG Da-wei(张大伟)^{1,2,3}, YANG Chen-ge(杨晨戈)², DAI Jun(戴俊)²,
WEN Jian-wu(温建武)¹, WANG Long(汪龙)¹, CHEN Chun-hua(陈春华)¹

1. Department of Materials Science and Engineering, University of Science and Technology of China,
Hefei 230026, China;

2. School of Chemical Engineering, Hefei University of Technology, Hefei 230009, China;

3. Anhui Key Laboratory of Controllable Chemistry Reaction and Material Chemical Engineering,
Hefei University of Technology, Hefei 230009, China

Received 10 August 2009; accepted 15 September 2009

Abstract: Sn-Ni alloy films for Li-ion batteries were fabricated by electrochemical deposition with rough copper foils as current collectors. The influence of electrochemical-deposition temperature and heat treatment were also investigated. By galvanostatic cell cycling the film anodes can deliver a steady specific capacity. The morphological changes cause the differences in capacity retention. After farther heat treatment, the film anodes present a better cycle performance, with a specific capacity of 314 mA·h/g after 100 cycles. This high capacity retention can be due to its smooth, compact surface formed in the heat treatment process.

Key words: electrochemical deposition; Li-ion battery; capacity retention; heat treatment

1 Introduction

Lithium-ion batteries have been commercially used as a power supply for portable electronic devices, such as cells. To meet the rapidly increasing demand on specific energy density of Li-ion batteries for diverse applications, the exploitation of new electrode materials with better performances has become the key issue. Many kinds of materials, especially tin-based compounds have drawn considerable attention due to their much higher electrochemical capacity compared with the traditional graphic materials in Li-ion batteries[1–2]. However, large volume expansion and contraction during the charge–discharge cycling were still the obstacles for their commercialization[3]. In the approaches adopted to overcome the electrode deterioration, fabrication of Sn_xM_y intermetallic compounds is a promising strategy. In Sn_xM_y intermetallic compounds the electrochemical process in a lithium cell involves the displacement of Sn metal, which forms the desired lithium alloy, $\text{Li}_{4.4}\text{Sn}$, while the other metal, M, acts as an electrochemically inactive matrix to buffer the volume variations during the

alloying process. It has been demonstrated that these materials exhibited longer cycle ability than that of pure tin electrode. So, a number of methods were used to fabricate tin-based alloy materials, such as high-energy ball milling[4–7], chemical reduction in aqueous solution[8], sputtering deposition [9–10], and solid-state reaction[11–12].

Compared with these above ways, the electrochemical deposition technique is relatively simple and inexpensive, which provides an exquisite way to fabricate tin-based alloys with specific morphologies [13–23]. Using Cu foil as current collector in electrochemical deposition, HASSOUN et al[14] synthesized Sn-Ni film electrodes for Li-ion batteries which showed a capacity of 530 mA·h/g after 40 cycles. HASSOUN et al[24] also fabricated Ni-Sn nanostructured electrodes by a template synthesis procedure, which delivered a capacity of 500 mA·h/g after 200 cycles. KE et al[21] fabricated macroporous Sn-Ni film electrodes with polystyrene (PS) spheres as templates, which retained a capacity of 500 mA·h/g after 70 cycles.

In this work, rough copper foils were chosen as current collectors, fabricating compact Sn-Ni film

electrode for Li-ion batteries by electrochemical deposition. The influence of heat treatment was also investigated. The integrity of the film electrode after electrochemical cycle and the influence of the electrode expansion were discussed.

2 Experimental

2.1 Fabrication of tin-based alloy film electrode by electrochemical deposition

The electrodeposition solution was comprised of $\text{SnCl}_2 \cdot 2\text{H}_2\text{O}$ (30 g/L), $\text{NiCl}_2 \cdot 6\text{H}_2\text{O}$ (22 g/L), $\text{K}_4\text{P}_2\text{O}_7 \cdot 3\text{H}_2\text{O}$ (150 g/L) and additive agent (10 g/L). All these reagents are of analytical grade. The pH value of the solution was adjusted to 8 by adding ammonia slowly. Then, a commercial copper foil was cleaned with absolute ethanol to serve as the working electrode in a two-electrode electrochemical cell, and a graphite plate was used as the counter electrode. Sn-Ni films were electrochemically deposited at a constant current density of 5 mA/cm^2 for 20 min in a glass cell at room temperature, which was strictly controlled by a potentiostat/galvanostat (HDV-7C). After deposition, the copper foil with Sn-Ni film was rinsed with absolute ethanol and then dried in air at room temperature for further analysis. It has been measured that the mass of the deposited Sn-Ni alloy film is about 1.1 mg with a thickness of about $2 \mu\text{m}$.

The influence of electrochemical-deposition temperature and heat treatment on synthesis of Sn-Ni film at 50°C in the electrochemical-deposition process was investigated. At the same time, the Sn-Ni films obtained at room temperature were sintered at 200°C for 2 h. Three different electrode samples were prepared and named NiSn-1(room temperature), NiSn-2(50°C) and NiSn-3(200°C), respectively.

2.2 Electrochemical characterization of obtained Sn-Ni alloy films

The electrochemical performances of the three kinds of Sn-Ni alloy films were measured using two-electrode coin cells (CR2032) of the $\text{Li}|1 \text{ mol/L LiPF}_6 (\text{EC}):\text{DEC}=1:1)|\text{Sn-Ni}$. These CR2032 cells were assembled in an argon-filled glove box. Celgard 2400 microporous polypropylene membrane was used as separator. These cells were cycled galvanostatically between 0 and 1 V at room temperature on a multi-channel battery test system (NEWARE BTS-610) to analyze the electrochemical responses. The current density was 0.4 mA/cm^2 .

2.3 Morphological and structural characterization of Sn-Ni alloy films

The as-prepared samples were characterized by

scanning electron microscope (JEOL 6390), and X-ray diffractometer (XRD, Philips X'Pert Pro Super X-ray diffractometer, Cu K_α radiation). Also X-ray fluorescence spectroscopy (XRF, XRF-1800) was used to make certain the surface composition.

The evolution of the crystalline form and morphology of the electrode material during cell cycling were determined by means of an EX situ X-ray diffractometer (XRD) and scanning electron microscope (SEM). The assembled coin cells were firstly discharged and charged to different stages on the battery test system and then opened in the glove box. The electrodes were washed with diethyl carbonate (DEC), sealed in thin, transparent polyethylene bags, respectively, and then delivered to the test of SEM.

3 Results and discussion

3.1 Structure and morphology of as-deposited Sn-Ni alloy electrode

The XRD patterns of the as-deposited Sn-Ni alloy electrodes are shown in Fig.1. As expected for samples prepared for electrodeposition, the peaks of all samples can be ascribed to both Ni_3Sn_4 phase and Ni_xSn_y metastable phase according to literature data[14]. The diffraction peak at 28° disappeared in NiSn-3 sample, which should be due to the result of reaction at 200°C . From the X-ray fluorescence spectroscopy, the Sn-Ni alloy electrode was composed of 71% Sn and 29% Ni (in mass fraction), which should be corresponding to Ni_3Sn_4 according to the molar ratio.

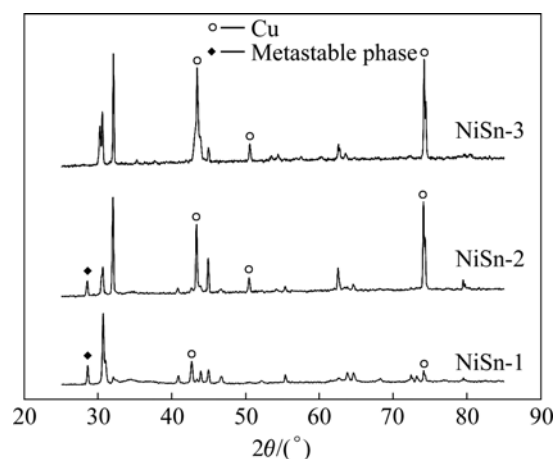


Fig.1 XRD patterns of Sn-Ni alloy films synthesized by electrochemical deposition at different temperatures room temperature

Fig.2 and Fig.3 show the morphologies of the three as-deposited Sn-Ni alloy films with the Cu foil as working electrode. Obvious differences among the samples can be observed. As shown in Fig.2(a), sample

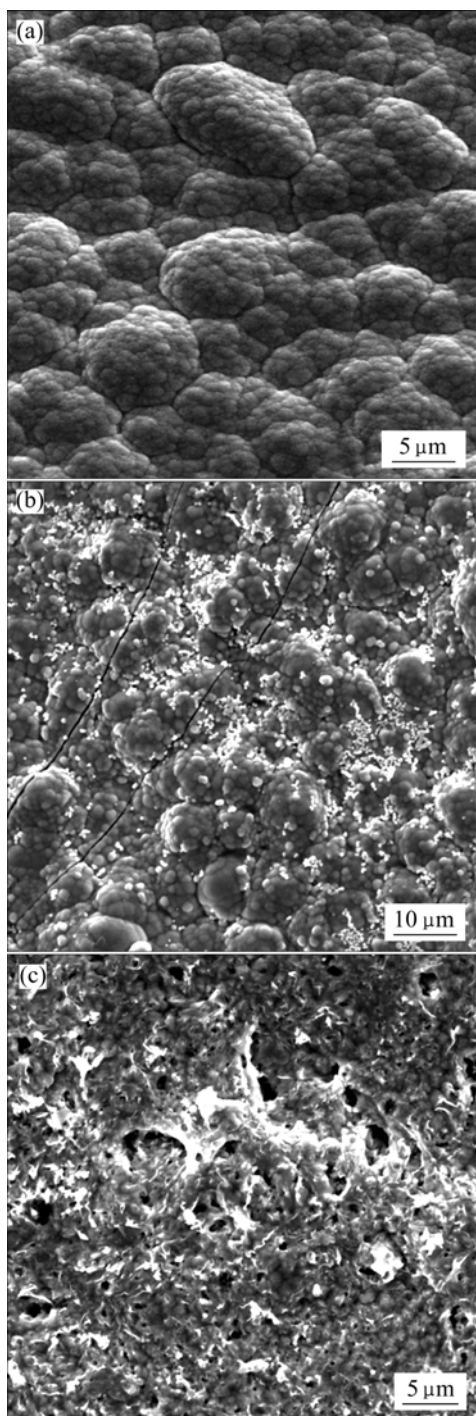


Fig.2 SEM images of as-deposited Sn-Ni alloy films: (a) NiSn-1; (b) NiSn-2; (c) NiSn-3

NiSn-1 has a compact, cauliflower-like morphology consisting of pillars formed by aggregates of small grains. The active material has a dense structure, and covers the Cu foil without any gaps and voids. However, this morphology gradually changes for the samples electrodeposited at different temperatures. In the sample NiSn-2 obtained at 50 °C, the surface is less dense due to some excess, small particles appearing on the top of the pillars. After being heated at 200 °C, the

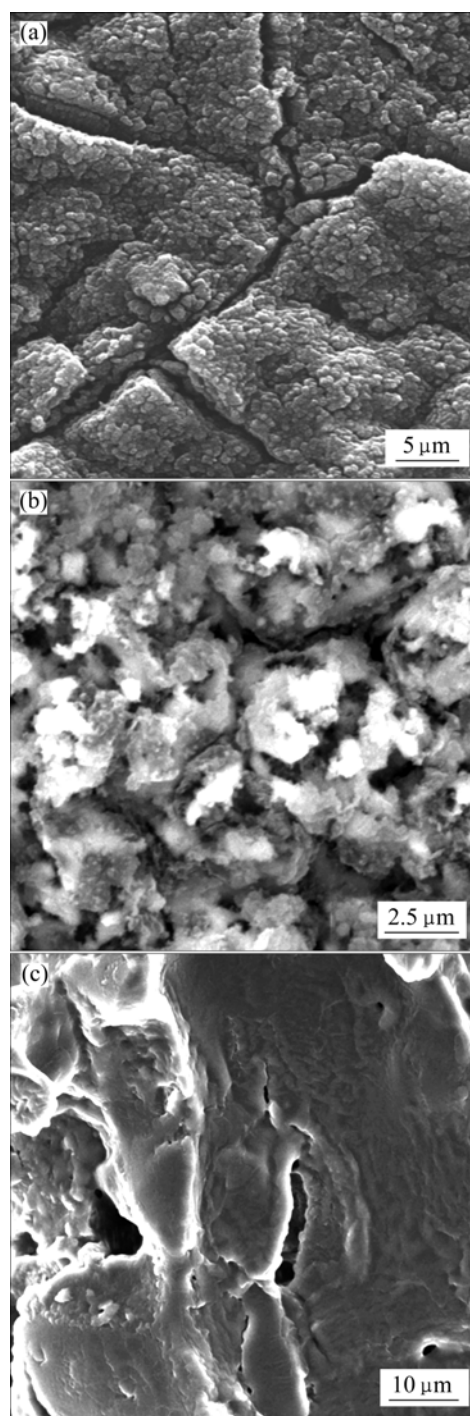


Fig.3 SEM images of Sn-Ni alloy film after discharge: (a) NiSn-1 after 60 cycles; (b) NiSn-2 after 40 cycles; (c) NiSn-3 after 1 000 cycles

pillars are “polished”, as shown in Fig.2(c). This should be due to re-reaction under the melting condition at 200 °C.

3.2 Electrochemical performances of Sn-Ni alloy electrode in lithium batteries

Fig.4 shows the voltage versus capacity profiles of the Sn-Ni/Li cells at 0.2C cycling rate. For sample NiSn-1(Fig.4(a)), the first discharge capacity of Sn-Ni

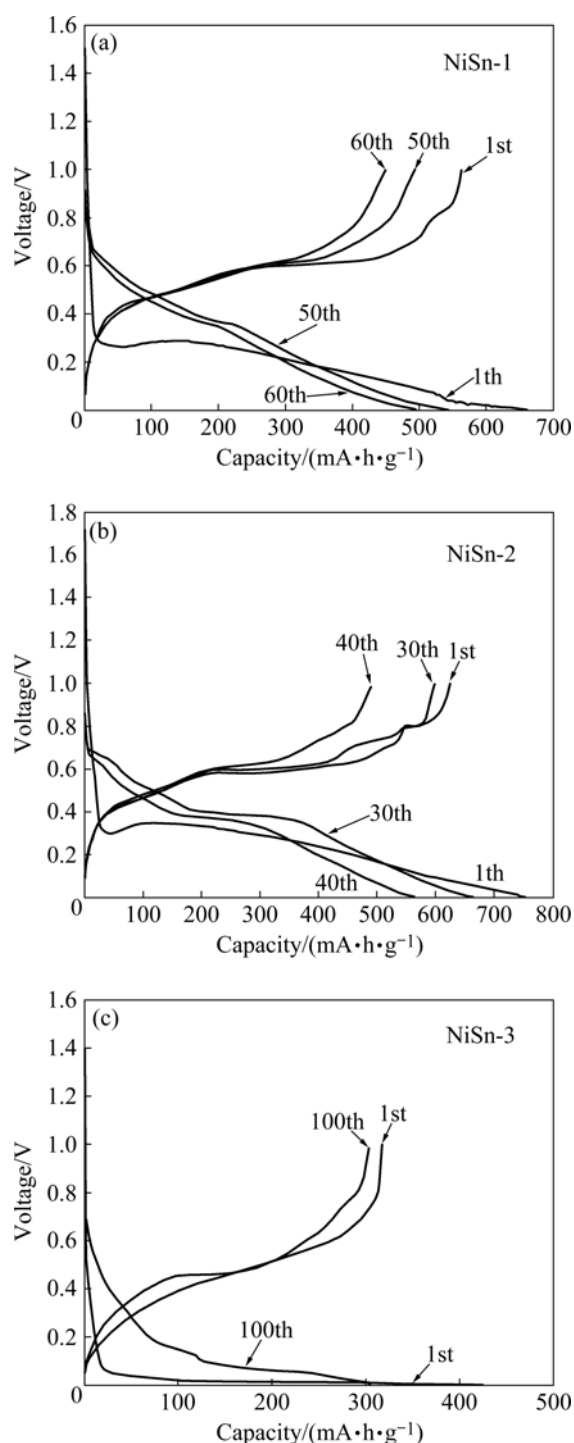


Fig.4 Voltage vs capacity profiles for the first discharge (Potential range of open circuit voltage to 0 V at current of 0.4 mA/cm²) and subsequent cycles (Potential range of 0–1 V, at current of 0.4 mA/cm²): (a) NiSn-1; (b) NiSn-2; (c) NiSn-3

alloy electrode is 660 mA·h/g, corresponding to a consumption of 16.1 Li⁺ per Ni₃Sn₄ formula. This consumption is lower than the theoretical value of 17.6 Li. The main reduction reaction in the first discharge process takes place at a low plateau of 0.25 V, while in the following discharge processes there are slope

plateaus beginning at 0.4 V. The capacity retention is 87% after the second discharge since 15.4 Li is consumed in the second discharge process. This sample delivers a capacity of about 550 mA·h/g after 50 cycles, with a capacity retention of 83%. But the slow capacity fading begins from the 50th cycle and the capacity keeps at 500 mA·h/g after 60 cycles. For sample NiSn-2(Fig.4(b)), the first discharge capacity of Sn-Ni alloy electrode is 754 mA·h/g, corresponding to a consumption of 18.4 Li⁺ per Ni₃Sn₄ formula. This consumption is higher than NiSn-1 or the theoretical value of 17.6 Li. This sample delivers a capacity of about 665 mA·h/g after 30 cycles, but the slow capacity fading begins from the 30th cycle and the capacity keeps at 563 mA·h/g after 40 cycles. For sample NiSn-3(Fig.4(c)), the first discharge capacity of Sn-Ni alloy electrode is only 425 mA·h/g, much lower than NiSn-1 or NiSn-2. But this sample delivers a steady capacity even after 100 cycles.

The electrochemical performances of the three samples are also shown in Fig.5. The first discharge capacity of NiSn-2 electrode is the highest, but the capacity fading begins from the 30th cycle. The first discharge capacity of NiSn-3 electrode is the lowest, but it delivers a steady capacity (314 mA·h/g) even after 100 cycles.

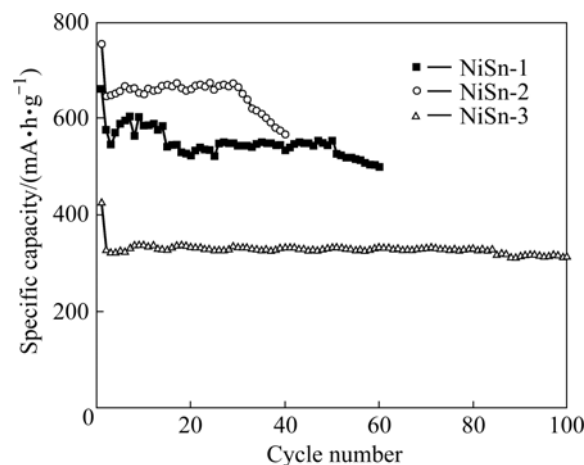


Fig.5 Specific capacity as function of cycle number for Sn-Ni/Li cells (Charge-discharge in voltage range of 1.0–0 V at 0.4 mA/cm²)

By combining with the surface morphologies in Fig.2 and Fig.3, the electrochemical differences of the three samples can be investigated. The surface structure of NiSn-2 is less dense and the aggregates of small grains are less compact. So, in the first discharge process the high surface area of the film enlarges to provide a larger reaction area and activate a less lithium-active portion of the film where Li⁺ is hardly diffused deeply in the film. This contributes to the high specific capacity in the first discharge process. But this film surface is more

incompact in the following electrochemical cycles, as shown in Fig.3(b), which leads to the mechanical disintegration of the electrode surface. The slow capacity fading begins from the 30th cycle, validating its poor cycle life.

By contrast with sample NiSn-2, sample NiSn-1 and NiSn-3 have compact film structures. Their film surfaces also keep integrity without active materials broke off from the copper current, as shown in Fig.3(a) and Fig.3(c). So, they can deliver steady capacity even after multi-cycle. Especially for sample NiSn-3, its surface is more smooth and the particles link each other compactly after being sintered at 200 °C. This structure is not easy to crack even after large volume change, which can take on a better buffer function than the other samples and avoid detrimental effect of volume changes of active materials during cycling, such as electrode pulverizing or capacity degrading. So, despite of its low capacity in the first discharge process, sample NiSn-3 shows excellent rate capability even after 100 cycles.

4 Conclusions

1) Using rough copper foils as current collectors, compact Sn-Ni film electrode for Li-ion batteries was fabricated by electrochemical deposition. The morphological changes deeply influence the electrochemical performances of the film electrode.

2) After heat treatment at 200 °C, this alloy film electrode has compact surface structure and keeps integrity after multi-electrochemical cycles. This alloy film electrode delivers a specific capacity of 314 mA·h/g even after 100 electrochemical cycles, which shows a good capacity retention.

References

- [1] COURTNEY I A, DAHN J R. Electrochemical science and technology electrochemical and in situ X-ray diffraction studies of the reaction of lithium with tin oxide composites [J]. *J Electrochem Soc*, 1997, 144(6): 2045–2052.
- [2] IDOTA Y, KUBOTA T, MATSUFUJI A, MAEKAWA Y, MIYASAKA. Tin-based amorphous oxide: A high-capacity lithium-ion-storage material [J]. *Science*, 1997(2): 1395–1397.
- [3] COURTNEY I A, DAHN J R. Key factors controlling the reversibility of the reaction of lithium with SnO₂ and Sn₂BPO₆ glass [J]. *J Electrochem Soc*, 1997, 144(9): 2943–2948.
- [4] FERGUSON P P, TODD A D W, DAHN J R. Comparison of mechanically alloyed and sputtered tin-cobalt-carbon as an anode material for lithium-ion batteries[J]. *Electrochem Commun*, 2008, 10(1): 25–31.
- [5] HASSOUN J, OCHAL P, PANERO S, MULAS G, MINELL C B, SCROSATI B. The effect of CoSn/CoSn₂ phase ratio on the electrochemical behaviour of Sn₄₀Co₄₀C₂₀ ternary alloy electrodes in lithium cells [J]. *J Power Sources*, 2008, 180(1): 568–575.
- [6] HASSOUN J, MULAS G, PANERO S, SCROSATI B. New electrochemical process for the in situ preparation of metal electrodes for lithium-ion batteries [J]. *Electrochem Commun*, 2007, 9(6): 2075–2081.
- [7] ZHANG J J, XIA Y Y. Co-Sn alloys as negative electrode materials for rechargeable lithium batteries [J]. *J Electrochem Soc*, 2006, 153(8): A1466–A1471.
- [8] WANG F, ZHAO M S, SONG X P. Nano-sized SnSbCu_x alloy anodes prepared by co-precipitation for Li-ion batteries [J]. *J Power Sources*, 2008, 175(1): 558–563.
- [9] TODD A D W, MAR R E, DAHN J R. Tin-transition metal-carbon systems for lithium-ion battery negative electrodes [J]. *J Electrochem Soc*, 2007, 154(6): A597–A604.
- [10] SHIEH D T, YIN J T, YAMAMOTO K, WADA M, TANASE S, SAKAIA T. Surface characterization on lithium insertion/deinsertion process for sputter-deposited AgSn thin-film electrodes by XPS [J]. *J Electrochem Soc*, 2006, 153(1): A106–A112.
- [11] SIMONIN L, LAFONT U, KELDER E M. SnSb micron-sized particles for Li-ion batteries [J]. *J Power Sources*, 2008, 180(2): 859–863.
- [12] GUO H, ZHAO H L, JIA X D, HE J C, QIU W H, LI X. A novel Sn₂SbNi composite as anode materials for Li rechargeable batteries [J]. *J Power Sources*, 2007, 174(2): 921–926.
- [13] ZHAO H P, JIANG C Y, HE X M, REN J G, WAN C R. Advanced structures in electrodeposited tin base anodes for lithium ion batteries [J]. *Electrochim Acta*, 2007, 52(28): 7820–7826.
- [14] HASSOUN J, PANERO S, SCROSATI B. Electrodeposited Ni-Sn intermetallic electrodes for advanced lithium ion batteries [J]. *J Power Sources*, 2006, 160(2): 1336–1341.
- [15] ARBIZZANI C, LAZZARI M, MASTRAGOSTINO M. Lithiation/delithiation performance of Cu₆Sn₅ with carbon paper as current collector [J]. *J Electrochem Soc*, 2005, 152(2): A289–A294.
- [16] SHIN H C, LIU M L. Three-dimensional porous copper-tin alloy electrodes for rechargeable lithium batteries [J]. *Adv Funct Mater*, 2005, 15(4): 582–586.
- [17] WANG L B, KITAMURA S, SONODA T, OBATA K, TANASE S, SAKAIA T. Electroplated Sn-Zn alloy electrode for Li secondary batteries [J]. *J Electrochem Soc*, 2003, 150(10): A1346–A1350.
- [18] TAMURA N, FUJIMOTO M, KAMINO M, FUJITANI S. Mechanical stability of Sn-Co alloy anodes for lithium secondary batteries [J]. *Electrochim Acta*, 2004, 49(12): 1949–1956.
- [19] TAMURA N, KATO Y, MIKAMI A, KAMINO M, MATSUTA S, FUJITANI S. Study on Sn-Co alloy electrodes for lithium secondary batteries II. Nanocomposite system [J]. *J Electrochem Soc*, 2006, 153(12): A2227–A2231.
- [20] TAMURA N, KATO Y, MIKAMI A, KAMINO M, MATSUTA S, FUJITANI S. Study on Sn-Co alloy anodes for lithium secondary batteries I. Amorphous system [J]. *J Electrochem Soc*, 2006, 153(8): A1626–A1632.
- [21] KE F S, HUANG L, JIANG H H, WEI H B, YANG F Z, SUN S G. Fabrication and properties of three-dimensional macroporous Sn-Ni alloy electrodes of high preferential (110) orientation for lithium ion batteries [J]. *Electrochem Commun*, 2007, 9(2): 228–232.
- [22] KE F S, HUANG L, CAI J S, SUN S G. Electroplating synthesis and electrochemical properties of macroporous Sn-Cu alloy electrode for lithium-ion batteries [J]. *Electrochim Acta*, 2007, 52(24): 6741–6747.
- [23] KE F S, HUANG L, WEI H B, CAI J S, FAN X Y, YANG F Z, SUN S G. Fabrication and properties of macroporous tin-cobalt alloy film electrodes for lithium-ion batteries [J]. *J Power Sources*, 2007, 170(2): 450–455.
- [24] HASSOUN J, PANERO S, SIMON P, TABERNA P L, SCROSATI B. High-rate, long-life Ni-Sn nanostructured electrodes for lithium-ion batteries [J]. *Adv Mater*, 2007, 19(3): 1632–1635.

(Edited by YANG Hua)